Journal of Materials Chemistry A

Accepted Manuscript

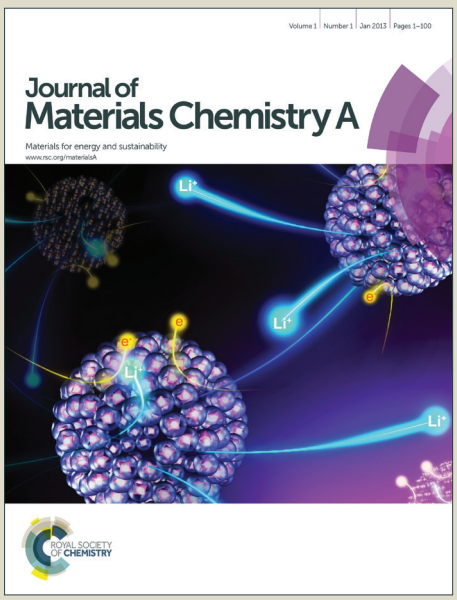

ROYAL SOCIETY OF CHEMISTRY

www.rsc.org/materialsA

Journal Name

RSCPublishing

Full Paper

Cite this: DOI: 10.1039/x0xx00000x

Received 00th January 2012,
Accepted 00th January 2012

DOI: 10.1039/x0xx00000x

www.rsc.org/

Solvent-mediated directionally self-assembling MoS_2 nanosheets to a novel worm-like structure and its application in sodium batteries

Maowen Xu[a,b,†], FengLian Yi[a,b,†], Yubin Niu[a,b], Jiale Xie[a,b], Junke Hou[a,b], Chuanjun Cheng[a,b], Sangui Liu[a,b], WeiHua Hu[a,b], Yutao Li[c], Chang Ming Li[a,b,*]

Ultralong worm-like MoS_2 nanostructures were assembled with solvent-mediation solvothermal process by controlling the composition ratio of the miscible precursors in solution. The forming mechanism of worm-like MoS_2 nanostructures was proposed and the as-prepared materials as anodes in sodium ion batteries delivered a good discharge/charge capacity, superior cycling stability and excellent coulombic efficiency. This work provides an efficient and economic approach to tailor the nanostructure of layered transition metal oxides and transition-metal dichalcogenide simply by controlling chemical composition and physical properties in a sovothermal process.

Introduction

For more than 20 years rechargeable lithium ion batteries have been widely used for portable electronic devices，power tools, hybrid/pure electric vehicles and electrical energy storage devices[1,2,3]. With depleting of lithium resources, however, concerns over the sustainable supply of lithium and increased lithium price[4-6] have arisen. In recent years, sodium-ion batteries have been extensively investigated owing to sodium's high abundance and low cost as well as the similarity of their solid-state electrochemistries with that of the Li-ion battery system.[7] Na ion has a larger ionic radius than that of Li-ion, which makes it more difficult to find a suitable host material to allow reversible and rapid ion insertion and extraction. Researchers have proposed a number of sodium anode electrode materials such as hard carbon and alloying compounds. Hard carbon has been used as the most common alternative anode material, but its capacity is severely limited by the applied current density[8]. Alloying compounds demonstrate high first cycle Na-storage capacities, and a very high volume change upon Na insertion, resulting in the formation of internal cracks, loss of electrical contact, and eventually a failure of the electrode.[9] Therefore, it is necessary to seek for reversible electrode materials with a higher stable cycle and a lower volume change. Besides carbon-based materials, other 2-D layered nanomaterials with large interlayer spacings have drawed much attention.[10-14] Molybdenum disulfide (MoS_2), a layered transition-metal dichalcogenide (TMD) in which hexagonal layers of Mo are sandwiched between two S layers, has been widely used as a functional material in such diverse fields as lubrication,[15] electronic transistors,[16] photovoltaics,[17] catalysis,[18] and batteries.[19,20] Its unique mechanical, optical and electrical properties are based on its chemical peculiarities. Strong covalent bonding characterizes the

Mo–S interactions, while 2D S–Mo–S layers are separated by weak van der Waals interactions. So it tends to form thin nanosheets. A variety of appealing strategies have been developed to prepare different morphologies of nanoscaled MoS_2. Nanowires,[21] nanotubes,[22] nanoribbons,[23] bubbles,[24] nanopods,[25] microspheres[26] and porous structures[27] have been reported. To the best of our knowledge, the synthesis of worm-like MoS_2 structure composed of ultrathin nanosheets performed in our lab was reported for the first time.

In this work, we develop a simple solvothermal approach that is designed to synthesize ultralong worm-like MoS_2 by self-assembling MoS_2 nanosheets under solvent mediation by controlling the composition ratio of the miscible precursor solution. The formating mechanism of MoS_2 under different conditions is proposed. The as-prepared worm-like MoS_2 with a well-ordered hierarchical structure showed a high reversible capacity, superior cycling stability and excellent coulombic efficiency when used as the anode electrode for sodium-ion batteries.

Experimental Section

Material preparation: All used chemical reagents were analytical grade as received. In a typical preparation process, 4 mmol of sulfur powder were dispersed into 14 mL octylamine and mixed with 13 mL absolute ethanol in a 50 mL Teflon-lined autoclave, then sonicated for 1 hour. 0.25 mmol of $(NH_4)_6Mo_7O_{24}\cdot 4H_2O$ were completely dissolved in 3 mL deionized water, that was then added into the suspension solution and sonicated for 1 hour to form a well-dispersed suspension. The autoclave was sealed and heated at 180~240 °C in an oven for several hours, and then cooled down to room temperature. The as-prepared products were collected by filtration and washed several times with ethanol, and then dried in vacuum at 100 °C overnight. In order to investigate the forming mechanism of the worm-like MoS_2, samples were also prepared by following the same experimental procedure as mentioned above just change different solvents ratio as listed in Table 1.

Table 1. Volume ratio of solvents in precursor solutions

Solution Vol . (ml) / Sample No. / Solution Type	I	II	III	IV
Octylamine	**0**	**14**	**14**	**30**
Absolute Ethanol	**0**	**13**	**0**	**0**
Deionized Water	**30**	**3**	**16**	**0**

Material characterization: The crystal structures of the materials were analyzed with a Philips X-ray diffractometer and Cu K-alpha radiation (λ=1.5406 nm) over the 2θ range of 10°-80°. Morphology and microstructure of the as-prepared products were examined by field-emission scanning electron microscopy (FESEM, JSM-7800N) and transmission electron microscopy (TEM, JEM-2100). Raman spectra were obtained using a HORIBA Scientific LabRAM HR Raman spectrometer system equipped with a 532.4 nm laser as the exciting radiation. X-ray photoelectron spectroscopy (XPS) measurements were performed on a Thermo Scientific ESCALAB 250Xi electron spectrometer. Fourier transform-infrared (FT-IR) spectra were recorded using the Nicolet FTIR 6700 spectrophotometer (Thermo Nicolet).

Electrochemical measurements: The electrodes were fabricated by coating a slurry of an active material (80 wt%), carbon black (15 %) and polyvinylidenefluoride (PVDF) binder (5 wt%) mixed in N-methyl pyrolidine (NMP) onto a copper foil and then dried in vacuum at 120 °C for 12 h. CR3025 coin cells were used and self-assembled in an argon-filled glove box. Na foil was used as the counter electrode, Celgard 2400 as the separator, and 1 M $NaPF_6$ in the solution of fluoroethylene carbonate/dimethyl carbonate (FEC/DMC, 1:1 by volume) as the electrolyte. The assembly of the cells was carried out in a dry Ar-filled glove box. The cells were aged for several hours before charge–discharge to ensure the full absorption of the electrolyte into the electrodes. The cells were galvanostatically charged and discharged between 0.01 V and 3 V versus Na/Na^+ in a Land Instruments testing system.

Results and Discussion

Material Characterization

The crystal structure of the as-obtained samples was investigated by X-ray diffraction (XRD). Fig1(a) shows that the major detectable diffraction peaks can be readily indexed to the hexagonal phase MoS_2, which is consistent with the standard powder diffraction file of MoS_2 (JCPDS No. 37-1492). There are no obvious peaks from possible impurity phases such as S, MoO_x and etc., demonstrating that the MoS_2 material with high purity could be obtained through the present synthesis strategy. The strong (002) peak often signifies a well-stacked layered structure. However, there is no obvious (002) peak observed in the as-prepared samples, indicating that the MoS_2 obtained in our work is very thin layered graphene-like structure, [28,29] which are consistent with the FESEM results. The insert of Fig.1 (a) shows the typical crystal structure of MoS_2, each Mo (IV) center occupies a trigonal prismatic coordination sphere, that is bound to six sulfide ligands; each sulfur centre is pyramidal and is connected to three Mo centres; in this way, the trigonal prisms are interconnected to give a layered structure, wherein molybdenum atoms are sandwiched between layers of sulfur atoms.

Raman spectroscopy has been extensively used for the characterization of micro- / nanocrystals. Raman analysis

showed in Fig 1(b) further confirms that the pure phase MoS_2 was formed in our work. The typical peak, known as the E^1_{2g} peak, at 376.7 cm^{-1} originates from the vibration of Mo–S in-plane mode, and an A_{1g} peak near 401.4 cm^{-1} from out-of-plane vibrations is also observed, which are typical first-order Raman active modes E^1_{2g} and A_{1g} due to in-plane vibrational modes within the sulfur-molybdenum-sulfur layer.[30]

Further structural details and composition were obtained with XPS analysis. In Figure 1(c), the peaks at ca. 161.4 and 162.7 eV can be indexed to $S2p_{3/2}$ and $S2p_{1/2}$ binding energies, respectively. And besides, there are two strong peaks at ca. 228.5 and 231.9 eV, which can be attributed to $Mo^{4+}3d_{5/2}$ and $Mo^{4+}3d_{3/2}$ binding energies, respectively. [31] The wideangle XPS (Figure 4d) of the obtained samples shows the predominant presence of Mo, S, C, and N, O. Among these elements, S and Mo is derived from MoS_2, C and N from octylamine. And the O signal was probably due to the exposure of the samples to atmosphere before the XPS measurement.

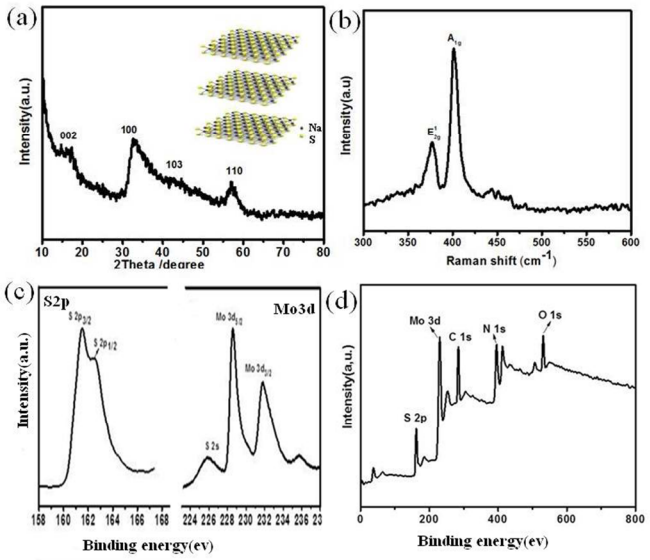

Figure 1. (a) XRD and (b) Raman spectra of the as-obtained sample. (c) S 2p and Mo 3d spectrum of as-obtained sample. (d) Wide survey XPS spectrum of MoS2 spectrum.

The morphology of the as-synthesized worm-like nanostructure was investigated by using FESEM and HRTEM, as shown in Fig 2 (a~f). Obviously, the worm-like MoS_2 are quite uniform, with length of over 10 μm and an average diameter of 200~300 nm (Fig 2b). Higher magnification FESEM images (Fig 2c) clearly revealed that the structure is composed of many individual thin round nanosheets, which have a highly ordered arrangement with all the sheets oriented parallel to each other. The TEM image further confirmed the well-defined nanosheet structure (Fig 2d). The high resolution image (Fig 2e) identified that the well-defined layered structures of MoS_2 having an interlayer distance of 0.61 nm for (200) planes have been observed. As shown in Fig. 2f, the existence of the MoS_2 phase was verified by clear ring diffraction patterns, which are indexed to a hexagonal *P63/mmc* space group and consistent with the XRD results.

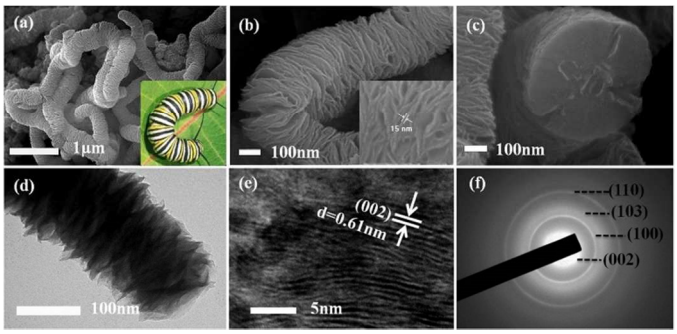

Figure 2. (a-c) FESEM, (d) TEM image, (e) HRTEM and (f) electron diffraction pattern of 3D MoS_2 of highly ordered hierarchical structures

In order to clearly understand the effect of solvents on the microstructures and morphologies of products, the samples prepared under same experimental process with different ratio of solvents were studied systemically in this work. As shown in Fig. 3, the XRD patterns of sample III and IV are in good agreement with that of sample II, demonstrating that high pure MoS_2 could be obtained in the solution of deionized water and octylamine and pure octylamine. Although some characteristic diffraction peaks of sample I can match well with the standard XRD pattern of MoS_2 (JCPDS No. 37-1492), there are still other diffraction peaks arising from the possible impurity phases such as MoO_x, due to lack protection of enough surface ligands.

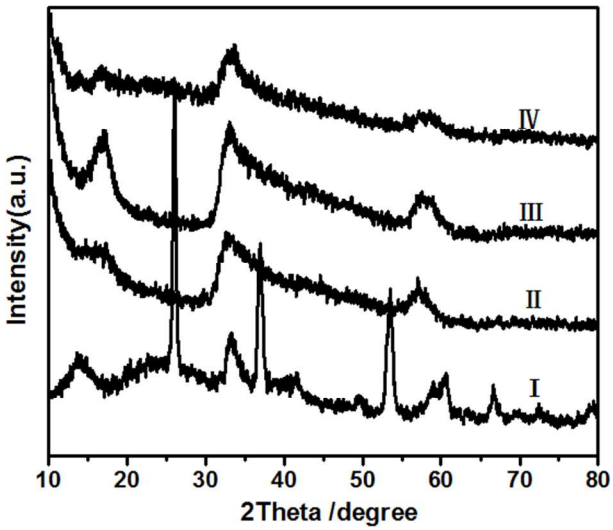

Figure 3. XRD patterns of samples obtained in the solvothermal process with solvents in different volume ratios

The as-prepared products were further examined by FESEM. As shown in Fig. 4, the microstructures and morphologies of the products formed under different conditions are very distinctive. The MoS_2 obtained from the pure aqueous solution are fluffy nanosheets (Fig 4a). Worm-like MoS_2 composing of ultrathin nanosheets was obtained in the solution of deionized water, octylamine and absolute ethanol (Fig. 4b). A structure of both worm-like MoS_2 and agglomerated bulks appeared in the samples obtained in the solution of deionized water and octylamine (Fig. 4c). With further increasing the viscosity of the precursor solution by only using octylamine as the solvent, agglomerated bulks became the main product (Fig. 4d).

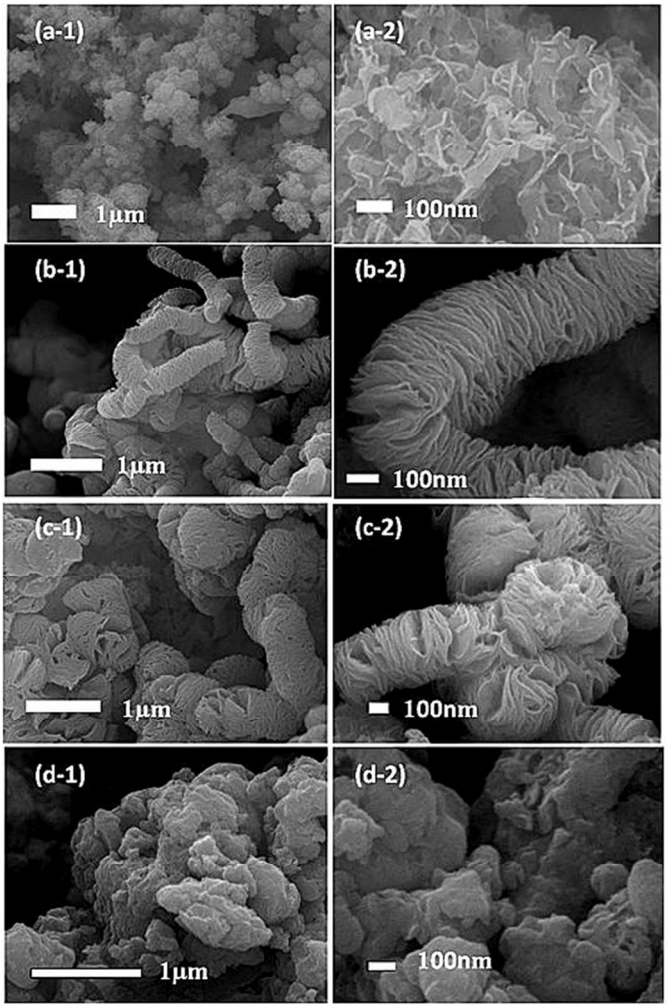

Figure 4. FESEM of samples obtained in precursor solutions with solvents in different volume ratios: low-magnification FESEM of samples (a-1) Ⅰ, (b-1) Ⅱ, (c-1) Ⅲ, (d-1) Ⅳ; high-magnification FESEM of samples (a-2) Ⅰ, (b-2) Ⅱ, (c-2)Ⅲ, (d-2)Ⅳ.

To further explore the growth mechanism of the worm-like MoS_2, time-dependent and temperature-dependent experiments were carried out. Fig. 5 (a~c) show the morphology evolution of the products obtained by just increasing the reaction time with other reaction conditions unchanged. It is clear that the worm-like structure could be formed within a short time (only 2 hours), and as the reaction time prolonged to 24 hours, the morphology of samples still keep unchanged. Fig 5 (d~f) show that worm-like products could also be formed at 180 °C, and at higher temperatures the morphology of the products has not been further improved and changed. Those results indicated that the process in which MoS_2 nanosheets were self-assembled into a worm-like structure is not controlled by thermodynamics or kinetics of the reaction involved and that the compositions of the miscible precursor solution play an important role in their assembling process.

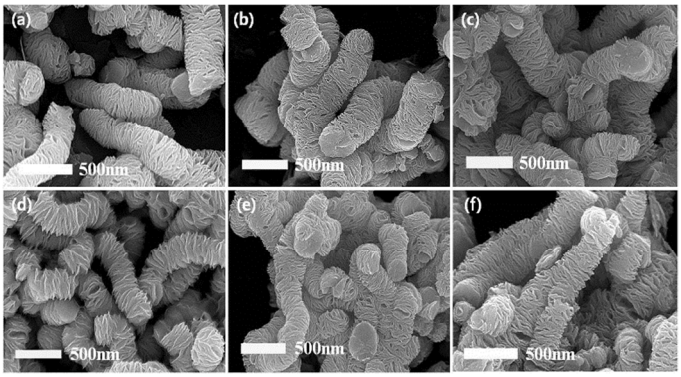

Figure 5. FESEM of samples obtained in the solvothermal process at 240 °C for different periods of time: (a) 2 h, (b) 6 h, (c) 12 h; and at different temperatures for 24 h: (d) 180 °C, (e) 200 °C, (f) 220 °C.

Mechanism Investigation

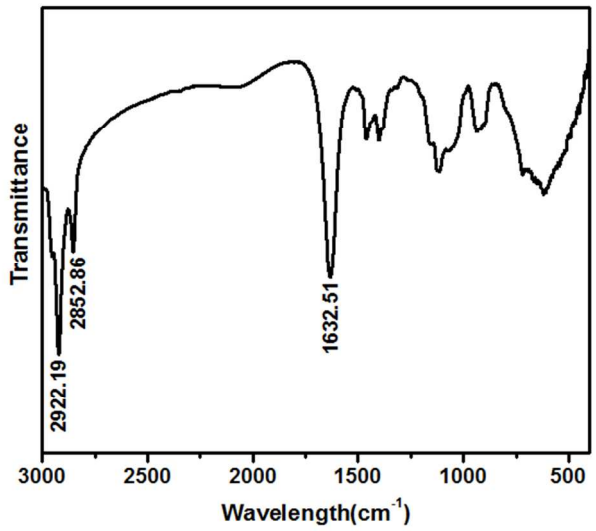

Figure 6. FT-IR spectrum of worm-like structures obtained in the solvothermal process

Octylamine coating the as-obtained sample was confirmed by FT-IR. As shown in Fig. 6, the CH_2 and CH_3 stretching vibrations at 2800–3000 cm^{-1} and N–H modes at 1650–1450 cm^{-1} (these peaks at 1650–1450 cm^{-1} may have overlapped with that of the bending vibration mode of H-O) in the FT-IR spectrum indicate that the products were capped with octylamine. The weight percent of the octylamine in the prepared samples was determined by TGA in air. The sharp drop in weight above 200 °C represents the decomposition and combustion of the octylamine and the phase transition of MoS_2 to MoO_3. Hence, the octylamine content in the as-synthesized sample is approximately 19.0 %. (As shown in Fig S1). On the basis of the FESEM, FTIR and TGA analyses, a possible mechanism is proposed to explain the formation of worm-like ultralong MoS_2 of a highly ordered hierarchical structure. In the MoS_2 synthesis reaction, the octylamine is served as a solvent and surface ligands. Functional groups $–NH_2$ of the octylamine molecule have a strong tendency to coordinate with inorganic cations and metals, as demonstrated by Burford and co-workers.[32,33] In the precursor solution of pure octylamine, due to the interaction $–NH_2$ with MoS_2, small MoS_2 nanosheets could aggregate together to produce sturdy agglomerated bulks (Fig. 4d). In the octylamine aqueous solution, the bonding force of $–NH_2$ with MoS_2 is weakened by the hydrogen-bonding between water and octylamine. So a well-ordered hierarchical structured 3D MoS_2 coexists with agglomerated bulks appears in the prepared samples (Fig. 4c). In the solution of octylamine, ethanol and water, the bonding force of $–NH_2$ is further weakened and then uniform 3D highly ordered hierarchical structured MoS_2 are obtained (Fig. 4b). When only using water as the precursor solution, the ultrathin and fluffy nanosheets are obtained since there are no $–NH_2$ groups on MoS_2 nanosheets. Thus it is rational that octylamine can intercalate MoS_2 layers to form worm-like ultralong MoS_2 with highly ordered hierarchical nanostructure. These results revealed that octylamine and the viscosity of the precursor solution play vital roles in creating worm-like ultralong MoS_2. The proposed mechanism is illustrated in Scheme 1.

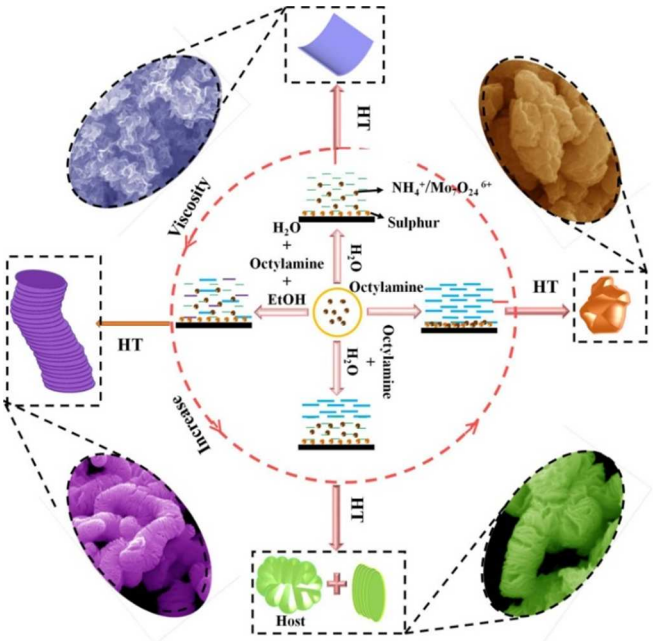

Scheme 1. Schematic illustration of the architecture mechanism for precursor solutions of solvents at different volume ratios

Electrochemical Performance

It is known that MoS_2 can be used as anode of sodium ion battery, Its typical electrochemical reaction in a Na battery proceed as following two steps[34,35]:

$$MoS_2 + xNa = Na_xMoS_2 \,(\text{above}\, 0.4, x < 2) \quad (1)$$

$$Na_xMoS_2 + (4 - x)Na = Mo + 2Na_2S (\text{below}\, 0.4V) \quad (2)$$

The electrochemical properties of the as-synthesized ultralong worm-like MoS_2 were examined to verify the advantages of this material as an anode material for Na-ion batteries as shown in Fig 7.

Fig 7a shows the charge/discharge behavior at the first, second, and third cycles of the as-obtained MoS_2 electrode between 3.0 and 0.01 V at a current density of 61.7 mA g^{-1}. In the first cycle, the MoS_2 electrode delivered a sodium insertion capacity of about 675.3 mAh g^{-1}, which is far higher than that of MoS_2 nanoflower (350 mAh g^{-1} at a current density of 50 mA g^{-1}) fabricated by Z. Hu et al.[34] Then it should be noted that the specific capacity fading in the first cycle is high up to 181.1 mA hg^{-1}, which may be caused by (i) the decomposition of the electrolyte on the surface of the MoS_2 to form a passivation layer, namely SEI film on the electrode and (ii) a fraction of Na^+ that was trapped in the nanoclusters or defect sites[36]. For the second and third cycles, charge and discharge capacities have no obvious fade, indicating that the stable SEI film has been formed after the first cycle. The cycling life of worm like MoS_2 with 80 cycles is shown in Fig. 7b. The discharge capacity after 80 cycles is 410.5 $mAhg^{-1}$, showing capacity retention of 83.1 %, compared with the second discharge. The average fade of subsequent specific capacity is just 0.21% per cycle. The stability and capacity of worm like MoS_2 is better than that of MoS_2 reported in literatures. [37, 38] Due to poor electrical conductivity of octylamine, the rate performance of the batteries is not good (as shown in Fig S2) and further improvement is undergoing in our lab. The high reversible capacity and good cycling stability of the as-synthesized ultralong worm-like MoS_2 electrodes demonstrate powerfully that the worm-like MoS_2 can be a promising alternative anode material for sodium ion batteries.

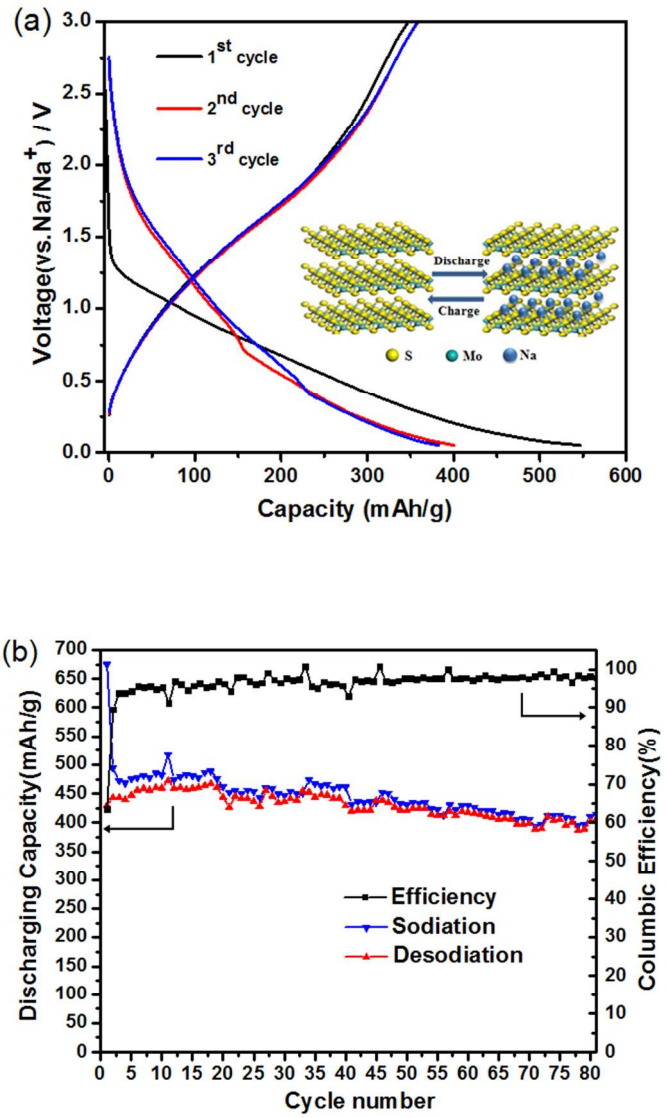

Figure 7. (a) Charge-discharge curves and (b) the cycling performance and their coulombic effciencies of the as-prepared MoS_2 for the potential window of 3.0~0.01 V vs Na/ Na^+.

Conclusions

In summary, ultralong worm-like MoS_2 nanostructures were assembled by a solution-mediation solvothermal process via controlling composition ratio of octylamine to water, the miscible precusors in solution to provide rational amount of ligands. The prepared material-based electrode with the ordered hierarchical structure delivered a capacity of 675.3 $mAhg^{-1}$ at discharge rates as high as 61.7 mAg^{-1} while possessing a capacity of 410.5 $mAhg^{-1}$ even after 80 cycles. Consequently, the significant contribution of this work provides not only an effective method for large-scale fabrication of worm-like ultralong MoS_2, but also a versatile strategy for further design and

development of layered transition metal oxides and transition-metal dichalcogenide.

Acknowledgement

This work is financially supported by Chongqing Key Laboratory for Advanced Materials and Technologies of Clean Energies under cstc2011pt-sy90001, Start-up grant under SWU111071 from Southwest University and Chongqing Science and Technology Commission under cstc2012gjhz90002. The work is also supported by grants from the National Natural Science Foundation of China (No. 21063014, 21163021), Fundamental Research Funds for the Central Universities (SWU113079, XDJK2014C051).

Notes and references

** Corresponding author*
[a]Institute for Clean Energy & Advanced Materials, Faculty of Materials and Energy , Southwest University, Chongqing 400715, P.R. China
[b]Chongqing Key Laboratory for Advanced Materials and Technologies of Clean Energies, Chongqing 400715, P.R. China
[c]Texas Materials Institute, University of Texas at Austin, Texas 78712, USA
† Maowen Xu and Chuan-Jun Cheng contributed equally to this work.
Fax: +86-23-68254969; Tel:+86-23-68254969;
E-mail:ecmli@swu.edu.cn

[1] D. Larcher, S. Beattie, M. Morcrette, K. Edstroem, J. C. Jumas, J. M. Tarascon, J. Mater.Chem. 2007, 17, 3759.

[2] J. B. Goodenough, Y. Kim, Chem. Mater. 2010, 22, 587.

[3] V. Etacheri, R. Marom, R. Elazari, G. Salitra, D. Aurbach, Energy Environ. Sci. 2011,4, 3243.

[4] M. Armand, J.M. Tarascon, Nature 2008, 451, 652.

[5] M.R. Palacin, Chem. Soc. Rev. 2009, 38, 2565.

[6] V. Palomares, P. Serras, I. Villaluenga, K. Hueso, J. Carretero-Gonzalez, T. Rojo, Energy Environ. Sci. 2012, 451, 5884.

[7] M. D. Slater, D. Kim, E. Lee and C. S. Johnson, Adv. Funct.Mater. 2013, 23, 947.

[8] S. M. Oh, S. T. Myung, C. S. Yoon, J. Lu, J. Hassoun, B. Scrosati,K. Amine, Y. K. Sun, Nano Lett. 2014, 14 (3), 1620.

[9] L. David, R. Bhandavat, G. Singh, ACS Nano 2014, 8(2), 1759.

[10] S. Yang, Y. Gong, Z. Liu, L. Zhan, D. P. Hashim, L. Ma, R. Vajtal, P. M. Ajayan, Nano Lett. 2013, 13 (4), 1596.

[11] M. Naguib, J. Halim, J. Lu, K. M. Cook, L. Hultman, Y. Gogotsi, M. W. Barsoum, J.Am. Chem. Soc. 2013, 135(43), 15966.

[12] a) M. Chhowalla, H. S. Shin, G. Eda, L. J. Li, K. P. Loh, H. Zhang, Nat. Chem. 2013, 5(4), 263.b) Z. Zeng, C. Tan, X. Huang, S. Bao, H. Zhang, Energy Environ. Sci. 2014, 7(2), 797.c) X. J. Wu, X. Huang, J. Liu, H. Li, J. Yang, B. Li, W. Huang, H. Zhang,Angew. Chem. Int. Edit. 2014, 126(20), 5183.d) D. Yang, Z. Lu, X. Rui, X. Huang, H. Li, J. Zhu, W. Zhang, Y. M. Lam, H. H.Hng,H. Zhang, Q. Yan, Angew.Commun. 2014, 126(35), 9506.

[13] X.S. Zhou, X. Liu, Y. Xu, Y.X. Liu, Z.H. Dai, and J.C. Bao, J. Phys. Chem. C. 2014, 118, 23527.

[14] X.S. Zhou, X.S. Zhu, X. Liu, Y. Xu, Y.X. Liu, Z.H. Dai, and J.C. Bao, J. Phys. Chem. C. 2014, 118, 22426.

[15] M. Chhowalla, G. A. J. Amaratunga, Nature 2000, 407, 164.

[16] B. Radisavljevic, A. Radenovic, J. Brivio, V. Giacometti, A. Kis,Nat. Nanotechnol. 2011, 6, 147.

[17] M. Fontana, T. Deppe, A. K. Boyd, M. Rinzan, A. Y. Liu, Sci. Rep. 2013, 3, 1634.

[18] H. I. Karunadasa, E. Montalvo, Y. Sun, M. Majda, J. R. Long, C. J. Chang, Science 2012, 335, 698.

[19] Y. Shi, Y.Wang, J. I.Wong, A. Y. S. Tan, C.-L. Hsu, L.-J. Li, Y.-C. Lu, H. Y. Yang, Sci. Rep. 2013, 3, 2169.

[20] Y. Chen, B. Song, X. Tang, L. Lu, J. Xue, Small 2014, 10(8), 1536.

[21] W. J. Li, E. W. Shi, J. M. Ko, Z. Z. Chen, H. Ogino, T. Fukuda, J. Cryst. Growth, 2003, 250, 418.

[22] K. P. Loh, H. Zhang, W. Z. Chen,W. Ji, J. Phys. Chem. B 2006, 110, 1235.

[23] Q. Li, J. T. Newberg, E. C. Walter, J. C. Hemminger, R. M. Penner, Nano Lett. 2004, 4, 277.
[24] I. Uzcanga, I. Bezverkhyy, P. Afanasiev, C. Scottand , M. Vrinat, Chem. Mater. 2005, 17, 3575.
[25] M. Remškar, A. Mrzel, M. Viršek, A. Jesih, Adv. Mater. 2007, 19(23), 4276.
[26] S. Ding, D. Zhang, J. S. Chen, X. W. D. Lou, Nanoscale, 2012, 4, 95.
[27] S. E. Skrabalak, K. S. Suslick, J. Am. Chem. Soc. 2005, 127, 9990.
[28] Y.C. Liu, L.F. Jiao, Q. Wu, J. Du, Y.P. Zhao, Y.C. Si,Y.J. Wang and H.T. Yuan, J. Mater. Chem. A. 2013, 1, 5822.
[29] K. Chang, W.X. Chen, L. Ma, H. Li, H. Li, F.H. Huang, Z.D. Xu, Q.B. Zhang and J.Y. Lee, J. Mater. Chem. 2011, 21, 6251.
[30] J. Kibsgaard, Z. Chen, B. N. Reinecke, T. F. Jaramillo, Nat. Mater. 2012, 11, 963.
[31] Q. Wang, J.H. Li, J. Phys. Chem. C. 2007, 111, 1675.
[32] B. Zhang,X.C.Ye,W.Y.Hou,Y. Zhao,Y.Xie, J. Phys. Chem. B. 2006, 110, 8978.
[33] S. J. Bao, C. M. Li, C. X. Guo, Y. Qiao, J. Power Sources 2008, 180(1), 676.
[34] Z. Hu, L.X.Wang, K. Zhang, J.B. Wang, F.Y. Cheng, Z.L. Tao, and J. Chen, Angew. Chem. 2014, 126, 1.
[35] L. David, R. Bhandavat, G. Singh, ACS Nano. 2014, 8, 1759.
[36] C. Feng , L.Huang , Z. Guo, H. Liu, Electrochem Commun.2007,9,119.
[37] Y.X. Wang, K. H. Seng, S.L. Chou, J.Z. Wang, Z.P. Guo, D. Wexler, H.K. Liu and S.X. Dou, Chem. Commun. 2014, 50, 10730.
[38] L. David, R. Bhandavat, and G. Singh, ACS Nano. 2014, 8 (2), 1759.